DOI: 10.1002/anie.201203007

Platinum-Catalyzed Asymmetric Hydrogenation: Spectroscopic Evidence for an O-H-O Hydrogen-Bond Interaction between Substrate and Modifier**

Fabian Meemken, Nobutaka Maeda, Konrad Hungerbühler, and Alfons Baiker**

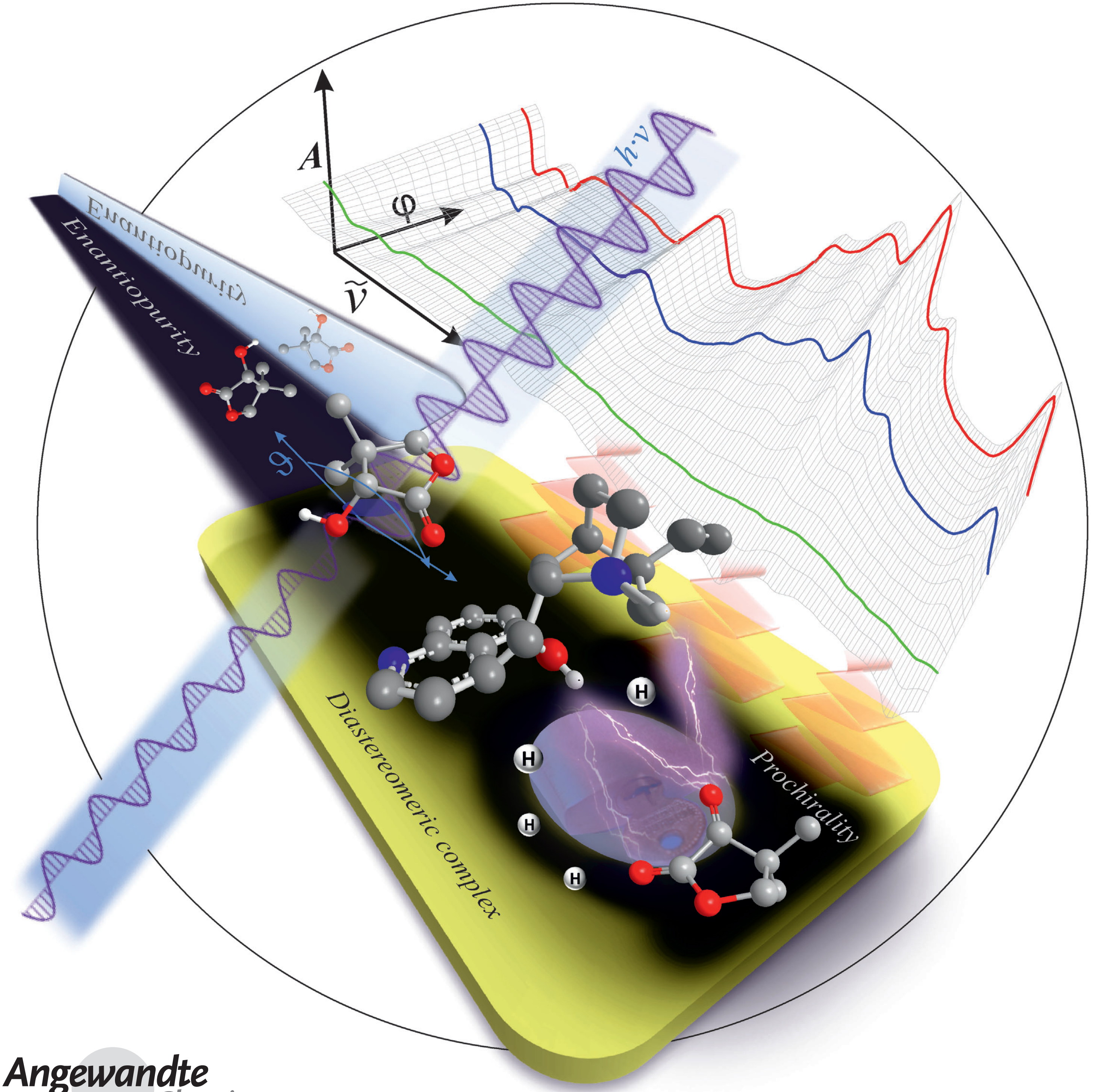

Enantiopurity is of crucial importance for the production of fine chemicals, pharmaceuticals, agrochemicals, flavors, and fragrances.[1] The great demand for, and the limited natural resources of optically active compounds have spurred research into their economical and sustainable production.[2] Among the strategies used for the production of pure enantiomers of a chiral product,[3] asymmetric catalysis plays a key role because of its efficiency and sustainability. While progress in homogeneous asymmetric catalysis has been remarkable,[4] advances in heterogeneous asymmetric catalysis have been rather limited,[5] mainly because of the inherent heterogeneity and complexity of chiral surfaces and that this area is much less researched. However, the application of heterogeneous asymmetric catalysis could be rewarding owing to inherent advantages it provides in separation, regeneration, and recycling of the catalyst, and the ease of transfer to continuous production processes.[6] Amongst the various strategies for designing heterogeneous enantioselective noble-metal catalysts,[7] the most efficient known today[8] is to bestow stereocontrol by adsorption of a suitable chiral auxiliary (modifier).[5] Simple addition of trace amounts of cinchona alkaloids to the reaction medium induces remarkably high enantiomeric excess (*ee*) in the hydrogenation of functionalized ketones on Pt catalysts (up to 98% *ee*).[9] However, in spite of the practical simplicity of this concept, the underlying mechanism is rather complex and only partly understood. A proper understanding of the enantiodifferentiating processes occurring at the chirally modified platinum surface is a basic requirement for understanding the mechanism of such reactions and the design of this type of catalysts. The aim of gaining a greater understanding has been pursued using both in situ spectroscopic studies on technical catalysts[10] as well as studies on well-defined single-crystal surfaces.[11] While investigations on single-crystal surfaces often allow gaining a deeper fundamental insight, in situ techniques can monitor the behavior of different components of the catalytic system under reaction conditions. Extensive studies have led to the proposal of several different mechanistic models for the platinum–cinchona system which have in common that the key feature is the role of the quinuclidine N-atom of the modifier in the enantioselection.[9c,12] The enantiodifferentiating interaction with the substrate is commonly proposed to originate from the tertiary amine functionality of the modifier, that is, from N-H-O type hydrogen bonding between the quinuclidine N-atom of cinchonidine (**2**) and the O atom of the keto carbonyl group. This assumption is supported by experimental findings, for example, N-substituted **2** affords only racemic yields (0% *ee*), whereas ether derivatives of **2** still offer stereocontrol for the hydrogenation of most ketones.[13] In a different model, two-point H-bonding interaction, was also proposed, assuming the N-H-O bonding between the quinuclidine N atom of **2** and the ester carbonyl O atom, and additional bifurcated H-bonding between two aromatic H atoms of **2** at 5′- and 6′-positions and the O atom of the keto carbonyl group.[12b,14] While the models for the diastereomeric complex show several common features they vary depending on the interacting substrate. For example, it seems that the diastereomeric complex formed during the hydrogenation of ketopantolactone (**1**) to (*R*)-pantolactone ((*R*)-**3**), an industrially important intermediate in the synthesis of pantothenic acid, cannot be described properly by the N-H-O interaction alone. Hydrogenation of **1** to (*R*)-**3** at room temperature and 70 bar in toluene affords 91.5% *ee* on **2**-modified Pt/Al_2O_3, whereas under the same condition the methyl ether derivative of **2**, MeO-**2**, yields considerably decreased *ee* values.[13,15] Furthermore, in contradiction to the proposed N-H-O interaction, N-substituted **2** still shows some enantioselection,[16] which might imply the involvement of another functional group of **2** in the enantiodifferentiating step.

Comparatively little attention has been given to the role of the C9-OH group of the cinchona modifier in the enantiodifferentiation, largely due to its weak acidity in solution. Very recently, the stereogenic center at C9 has been found to affect both rates and enantioselection in the hydrogenation of various ketones, including **1**.[17] Herein, we study the role of the C9-OH group in the enantiodifferentiating surface process using in situ ATR (attenuated total reflection) IR spectroscopy combined with modulation excitation spectroscopy (MES) and phase-sensitive detection (PSD), and provide the first experimental evidence for the formation of an O-H-O bonded surface diastereomeric intermediate complex between **1** and **2** under reaction conditions.

The combination of ATR-IR with MES is a powerful tool to explore the complex catalytic solid–liquid interface under reaction conditions.[18] It allows the discrimination between active species and spectators, and the elucidation of the structure and environment of molecular interactions. Additionally, mathematical transformation of the transient MES data from time- to phase-domain by PSD,[19] according to Equation (1), provides further sensitivity enhancement and kinetic insight, where T is the length of a cycle, ω is the demodulation frequency, φ_k is the demodulation phase angle, k is the demodulation index ($k=1$ in this study) and $A(t,\tilde{\nu})$ and $A_k(\tilde{\nu})$ are the active species responses in time- and phase-domain, respectively.

$$A_k(\tilde{\nu})\cos\left(\varphi_k + \varphi_k^{\mathrm{Delay}}(\tilde{\nu})\right) = \frac{2}{T}\int_0^T A(t,\tilde{\nu})\sin(k\omega t + \varphi_k)dt \qquad (1)$$

The time-resolved surface plot presented in Figure 1a displays molecular vibrations induced during adsorption of

---

[*] F. Meemken, Dr. N. Maeda, Prof. Dr. K. Hungerbühler,
Prof. Dr. A. Baiker
Department of Chemistry and Applied Biosciences
Institute for Chemical and Bioengineering
Hönggerberg, HCI, 8093 Zürich (Switzerland)
E-mail: nobutaka.maeda@chem.ethz.ch
alfons.baiker@chem.ethz.ch
Homepage: http://www.sust-chem.ethz.ch, www.baiker.ethz.ch

Prof. Dr. A. Baiker
Chemistry Department, Faculty of Science
King Abdulaziz University
P.O. Box 80203, Jeddah 21589 (Saudi Arabia)

[**] We thank Dr. Tamas Mallat (ETH Zurich) for valuable discussion.

Supporting information for this article is available on the WWW under http://dx.doi.org/10.1002/anie.201203007.

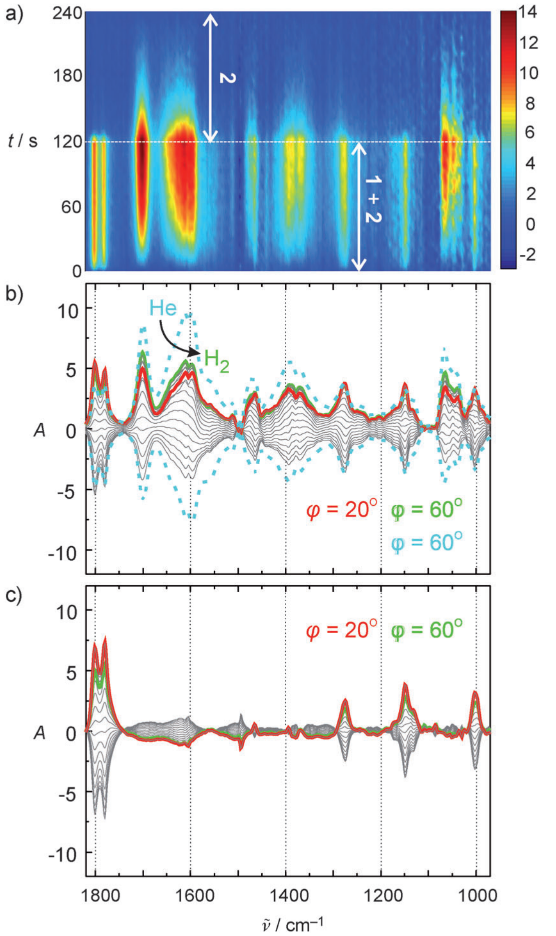

Figure 1. a) Time- and b, c) phase-resolved spectra during **1** concentration modulation between 0 and 1 mм on (a, b) **2**- and (c) MeO-**2**-modified Pt/Al$_2$O$_3$ in H$_2$-saturated (solid green lines) or He-saturated (dashed cyan line) toluene at 298 K. The absorbance values are divided by 10^{-4}.

1 and its interaction with the **2**-modified Pt surface. Upon admission of **1** solution, quick adsorption of the substrate is evident from strong absorption bands of C═O at 1800 (ester-carbonyl) and 1780 cm^{-1} (keto carbonyl group). Three bands at 1275, 1149, and 1003 cm^{-1} are also assigned to **1**. According to Greenler's surface selection rule the adsorbed rigid ring with its in-plane carbonyl groups cannot be perfectly parallel to the surface as the dipole moment changes of the observed vibrational modes would be cancelled out.[20]

After a short delay, new bands appeared at around 1700, 1610, 1470, 1390, and 1050 cm^{-1}. In contrast to the quickly saturated bands of **1**, the additional bands continuously increased and showed a significantly slower desorption process, indicating the formation of stable surface species. As seen in Figure 1 b, further analysis of the data in phase-domain (φ: 0→180°) gives clear evidence that all the additional bands obeyed the same kinetics ($\varphi = 60°$), following initially adsorbed **1** ($\varphi = 20°$). Hence, they must originate from restructuring of co-adsorbed **1** and **2**, slowly forming a surface diastereomeric intermediate complex, that is, **1**·**2**. Upon switching from He- to H$_2$-saturated solutions all signals of **1**·**2** decreased while features assigned to **1** did not alter. This situation is a clear indication for the saturation of the surface complex, the intermediate species, with dissociated hydrogen to produce **3**.

Interesting insight into the **1**·**2** interaction is given by the same experiment with MeO-**2** (Figure 1 c). The blocking of the alcohol function completely suppressed the formation of the intermediate complex. Clearly, the C9-OH group is involved in the formation of the surface complex with **1** through hydrogen bonding. Bands at 1700 and 1610 cm^{-1} for the surface complex (Figure 1 a,b) most likely originate from the two *cis*-carbonyl groups of **1**. Compared to the original **1** bands, both C═O bands were broadened, particularly the band at 1610 cm^{-1}. Since hydrogen bonding typically leads to peak broadening,[21] the interaction between carbonyl groups and C9-OH via O-H-O type H-bonding, that is, C9−O···H···O═C, is most feasible.

Further clarification of the role of the modifier in the surface complex is provided by the reverse MES experiments, that is, modulation of the concentration of **2** between 0 and 1 mм in the absence (Figure 2 a) and presence (Figure 2 b and c) of **1**. Different adsorption geometries of **2** have been detected on the Pt surface (Scheme 1); π-bonded **2** (species **2a**) and N-lone pair bonded **2** (species **2b**).

The spectral features differ only slightly, but they can be distinguished in the IR spectra through changes in the dynamic dipole moment of quinoline rings, which was also

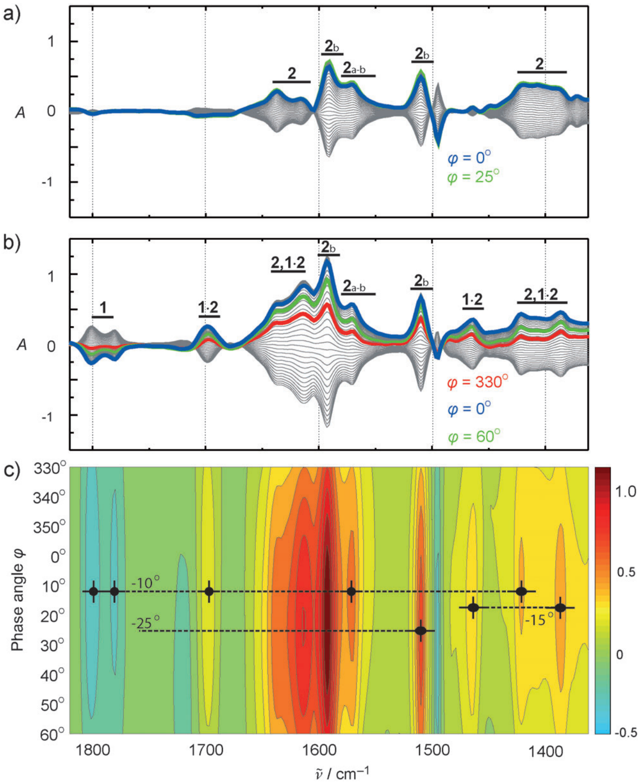

Figure 2. Demodulated (a,b) and phase-resolved (c) MES-spectra of the concentration modulation of **2** between 0 and 1 mм in H$_2$-saturated toluene in absence (a) and presence (b,c) of 1 mм **1** on Pt/Al$_2$O$_3$ at 298 K. The absorbance values are divided by 10^{-3}.

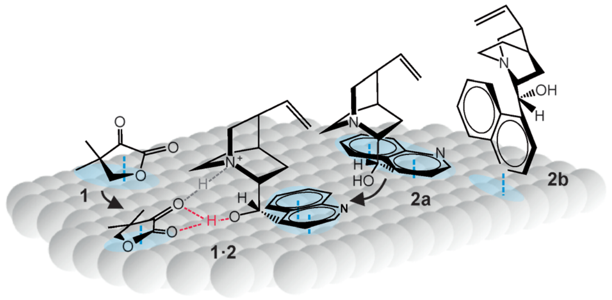

Scheme 1. Identified adsorbed molecules and their proposed interaction; **2a** = π-bonded **2**, **2b** = N-lone pair bonded **2**. For the sake of clarity the previously identified N-H-O interaction is omitted.

confirmed by ab initio calculations.[22] On the bare Pt surface (Figure 2a), both **2a** and **2b** obeyed the same kinetics ($\varphi = 25°$) during adsorption–desorption cycles. However, the kinetic process completely differed on the **1**-covered Pt surface. Upon admission of **2**, formation of the surface **1·2** complex is evident from appearance of its characteristic bands at 1700 and 1610 cm^{-1} and simultaneous attenuation of carbonyl signals from surface **1** (Figure 2b).

The detailed kinetic information regarding the complex formation can be better highlighted in the phase-angle resolved surface plot (Figure 2c). It is striking that species **1**, **2a**, and **3** (see Scheme 1) obeyed the same kinetics, that is, with a phase-delay $\varphi^{\text{Delay}} = -10°$. Hence, it can be inferred that **2** anchored to the surface with the quinoline-π-system interacted with an adjacently co-adsorbed **1** to form the **1·2** complex. Further increase in **2** coverage led to the formation of N lone-pair bonded **2** identified at $\varphi^{\text{Delay}} = -25°$, which seems not to be participating in the enantiodifferentiating step. The discrimination of N lone-pair bonded **2** as spectator is also in line with the observations during the **1** modulation experiment, since the peak observed at 1510 cm^{-1} emerged at $\varphi = 70°$ (see Figure 1b and Supporting Information). Scheme 1 provides an overview of the proposed mechanistic model for the formation of the surface **1·2** complex. Owing to the considerable red shifts of both carbonyl groups of **1**, it is reasonable to consider the involvement of both of them in the O-H-O type H-bonding interaction.

Finally, we address the key characteristic of an enantioselective catalytic system, the stereochemical control. For this purpose, we have investigated how the different enantiomeric products, (*R*)-**3** and (*S*)-**3**, affect the **1·2** complex formation. Figure 3 shows the particular enantiodifferentiation toward the right-handed enantiomer. The major product enantiomer (*R*)-**3** clearly interferes with the formation of the complex, and its competition for the chiral pocket in **2** is evident from the continuous removal of the associated bands. In contrast, (*S*)-**3** did not affect significantly the **1·2** complex formation.

In conclusion, our study provides the first in situ spectroscopic evidence for the possible role of the C9-OH functionality in cinchona alkaloids in the enantiodifferentiating diastereomeric complex formed between **2** and **1**. This observation extends the generally accepted model for enantiodifferentiation based on the formation of a H-bonding between the quinuclidine-N atom of the cinchona alkaloid and the oxygen of the α-carbonyl group of the ketone (N-H-O type H-bonding) and indicates that for some ketones the C9−O···H···O=C interaction has to be taken into account for explaining the enantiodifferentiation. As N-substituted **2** still shows enantioselection (inversed *ee* value, though),[16] we consider that the C9−O···H···O=C interaction plays an important role in the enantiodifferentiating step for the asymmetric hydrogenation of **1** on cinchona-modified Pt catalysts. A synergetic effect of both hydrogen-bonding interactions (N-H-O and C9−O···H···O=C) seems to be the origin of the high enantioselectivity achieved with **1** on cinchona-modified platinum. While the C9-OH group of the cinchona alkaloid does not appear to be crucial for the enantioselection in the hydrogenation of several α-ketoesters,[12d] it apparently cannot be ignored when explaining the enantiodifferentiation of **1**. This finding may help to refine the existing models of enantiodifferentiation for asymmetric hydrogenation of activated ketones on cinchona-modified platinum.

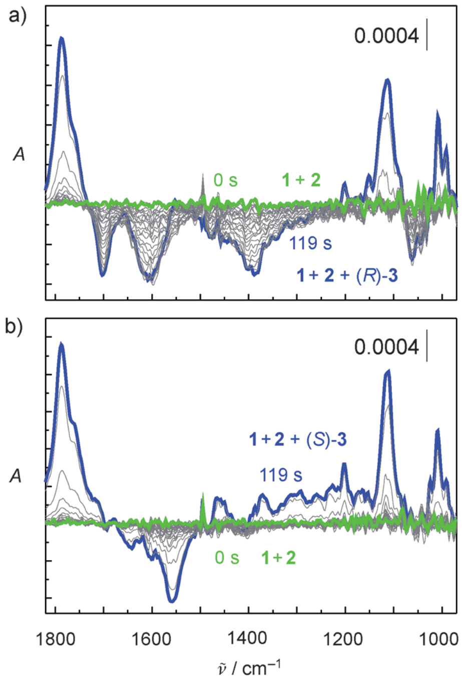

Figure 3. ATR-IR spectra during the addition of 1 mM of a) (*R*)-**3** and b) (*S*)-**3** addition to the flow after the saturation of the Pt/Al$_2$O$_3$ surface with a solution of 1 mM **2** and 1 mM **1** in He-saturated toluene at 298 K.

Experimental Section

A film of Pt/Al$_2$O$_3$ catalyst (BASF-Engelhard 4759) was deposited on an ZnSe internal reflection element (IRE, bevel of 45°, 52 mm × 20 mm × 2 mm, Crystran Ltd), and placed in a home-build flow-through cell. ATR-IR spectra were recorded on a Bruker IFS-66/S spectrometer equipped with a liquid-nitrogen cooled MCT (MTC = mercury cadmium telluride) detector at 4 cm^{-1} resolution. Modulation excitation experiments were carried out by changing between two different solutions every 119 s. The cycles were repeated eight times to obtain stable responses of active species, and the last five cycles were integrated into one cycle to average the spectra and to enhance the signal to noise ratio. Details of the experimental procedure are available in the Supporting Information.

Received: April 19, 2012

Keywords: asymmetric hydrogenation · IR spectroscopy · diastereomeric complex · heterogeneous catalysis · modulation excitation spectroscopy

---

[1] A. N. Collins, G. N. Sheldrake, J. Crosby, *Chirality in Industry: The Commercial Manufacture and Applications of Optically Active Compounds*, Wiley, New York, **1995**.

[2] S. C. Stinson, *Chem. Eng. News* **2001**, *79*, 35–38.

[3] R. A. Sheldon, *J. Chem. Technol. Biotechnol.* **1996**, *67*, 1–14.

[4] R. Noyori, T. Ohkuma, *Angew. Chem.* **2001**, *113*, 40–75; *Angew. Chem. Int. Ed.* **2001**, *40*, 40–73.

[5] H. U. Blaser, B. Pugin, F. Spindler, *J. Mol. Catal. A* **2005**, *231*, 1–20.

[6] N. Künzle, R. Hess, T. Mallat, A. Baiker, *J. Catal.* **1999**, *186*, 239–241.

[7] M. Heitbaum, F. Glorius, I. Escher, *Angew. Chem.* **2006**, *118*, 4850–4881; *Angew. Chem. Int. Ed.* **2006**, *45*, 4732–4762.

[8] A. Baiker, *Catal. Today* **2005**, *100*, 159–170.

[9] a) T. Mallat, E. Orglmeister, A. Baiker, *Chem. Rev.* **2007**, *107*, 4863–4890; b) H. U. Blaser, B. Pugin, F. Spindler, M. Thommen, *Acc. Chem. Res.* **2007**, *40*, 1240–1250; c) M. Bartók, *Curr. Org. Chem.* **2006**, *10*, 1533–1567; d) D. Y. Murzin, P. Maki-Arvela, E. Toukoniitty, T. Salmi, *Catal. Rev. Sci. Eng.* **2005**, *47*, 175–256; e) F. Zaera, *Acc. Chem. Res.* **2009**, *42*, 1152–1160.

[10] a) J. Kubota, F. Zaera, *J. Am. Chem. Soc.* **2001**, *123*, 11115–11116; b) N. Maeda, K. Hungerbühler, A. Baiker, *J. Am. Chem. Soc.* **2011**, *133*, 19567–19569.

[11] a) V. Demers-Carpentier, G. Goubert, F. Masini, R. Lafleur-Lambert, Y. Dong, S. Lavoie, G. Mathieu, J. Boukouvalas, H. Gao, A. Rasmussen, L. Ferrighi, Y. Pan, B. Hammer, P. McBreen, *Science* **2011**, *334*, 776–780; b) J. M. Bonello, R. M. Lambert, *Surf. Sci.* **2002**, *498*, 212–228.

[12] a) N. Bonalumi, T. Bürgi, A. Baiker, *J. Am. Chem. Soc.* **2003**, *125*, 13342–13343; b) S. Lavoie, G. Mahieu, P. H. McBreen, *Angew. Chem.* **2006**, *118*, 7564–7567; *Angew. Chem. Int. Ed.* **2006**, *45*, 7404–7407; c) J. L. Margitfalvi, E. Tfirst, *J. Mol. Catal. A* **1999**, *139*, 81–95; d) H. U. Blaser, H. P. Jalett, M. Muller, M. Studer, *Catal. Today* **1997**, *37*, 441–463; e) F. Zaera, *J. Phys. Chem. C* **2008**, *112*, 16196–16203.

[13] S. Diezi, A. Szabo, T. Mallat, A. Baiker, *Tetrahedron: Asymmetry* **2003**, *14*, 2573–2577.

[14] S. Lavoie, M. A. Laliberte, I. Temprano, P. H. McBreen, *J. Am. Chem. Soc.* **2006**, *128*, 7588–7593.

[15] M. Schürch, N. Künzle, T. Mallat, A. Baiker, *J. Catal.* **1998**, *176*, 569–571.

[16] E. Orglmeister, T. Mallat, A. Baiker, *J. Catal.* **2005**, *233*, 333–341.

[17] E. Schmidt, C. Bucher, G. Santarossa, T. Mallat, R. Gilmour, A. Baiker, *J. Catal.* **2012**, *289*, 238–248.

[18] A. Urakawa, T. Bürgi, A. Baiker, *Chem. Eng. Sci.* **2008**, *63*, 4902–4909.

[19] D. Baurecht, U. P. Fringeli, *Rev. Sci. Instrum.* **2001**, *72*, 3782–3792.

[20] R. G. Greenler, D. R. Snider, D. Witt, R. S. Sorbello, *Surf. Sci.* **1982**, *118*, 415–428.

[21] P. J. Larkin, *IR and Raman Spectroscopy: Principles and Spectral Interpretation*, Elsevier, Oxford, **2011**.

[22] D. Ferri, T. Bürgi, *J. Am. Chem. Soc.* **2001**, *123*, 12074–12084.